European Polymer Journal 164 (2022) 110888

Contents lists available at ScienceDirect

European Polymer Journal

journal homepage: www.elsevier.com/locate/europolj

Sequential and selective shape memory by remote electrical control

A. Cortés, N. Pérez-Chao, A. Jiménez-Suárez, M. Campo, S.G. Prolongo *

Materials Science and Engineering Area, University Rey Juan Carlos, C/Tulipán s/n, 28933 Móstoles, Madrid, Spain

ARTICLE INFO

Keywords:
Epoxy resin
Electro active actuators
Shape memory
Nanocomposite
Carbon nanotube
Joule effect

ABSTRACT

Shape memory (SM) materials have been widely investigated for several years. Most polymers present SM behaviour based on their thermo-mechanical properties. However, they are usually stimulated by an external heating source, hindering their industrial application. The addition of carbon nanotubes (CNT) allows turning conventional SM polymers into electro-active actuators. In this regard, the resistive heating by the Joule effect is considerably fast with a low energy cost.

The most used epoxy resins cured at high temperature are based on diglycidyl ether of bisphenol A (DGEBA) cured with aromatic amine hardeners, such as diaminodiohenylsulfone (DDS) and 4,4′diamine-diphenylmetane (DDM). In this work, they were synthesised with modification of the epoxy/amine ratio to vary the crosslinking density of networks so as to build up different viscoelastic properties in order to tailor their SM behaviour. Electrically conductive nanocomposites were manufactured by adding a CNT percentage above the percolation threshold.

A comparison of SM behaviour stimulated by traditional convection and resistive heating was carried out, confirming the higher recovery ratio, speed, and applicability of the electrical stimuli. In addition, the configuration of electrodes allows the design of self-deployable materials with remote control. In this way, the most common dual-shape SM polymers (one permanent shape and one temporary shape) can easily develop several stable temporary shapes. Moreover, the electrical remote control provides sequential and selective actuators, enhancing their performance for developing smart structures with shape memory capability.

1. Introduction

Actuators convert an external stimulus, such as heat, light or electrical current, into deformation output. Liquid crystal polymers, dielectric elastomers, and shape memory (SM) polymers are being widely investigated to develop actuators [1,2]. SM polymers are stimuli-responsive or smart materials, able to recover their original permanent shape upon exposure to external stimuli [3–5]. Most SM thermosetting polymers are thermally triggered. They are manufactured with a stable state shape (original shape) which is transformed into one or several unstable states (temporary shapes) by thermo-conforming. During the deformation by external load application, the network adopts a rearranged conformation, storing strain energy when it is cooled down. Then, when the stressed resin is heated, the stored energy is released, and the permanent shape is entropically restored. The switching or transition temperature of SM thermosets is usually their glass transition temperature (Tg). Numerous potential applications [6] are being designed for SM thermosets such as self-deployable aerospace structures, i.e., satellite panel trusses and solar sail boom structures, self-healing systems, remote medical instruments, bionic engineering, devices for energy, electronic and civil engineering, and household products, among others. However, in the most of them, thermal triggering could be an important limitation because of the need for using complicated external heating sources.

The addition of nanoparticles to SM thermosetting polymers is also being widely investigated [7–9]. Particularly, graphitic nanoparticles are added to increase the thermal conductivity of nanocomposites, increasing the thermal SM response speed [9] and enhancing the mechanical properties at temperatures close to Tg, which increases the repeatability of SM cycles [9,10]. Moreover, the recovery stress [10] is much larger than neat SM resins. Therefore, SM nanocomposites have further enhanced and broadened applications. The nanofiller addition can enable a thermal stimulation [7], turning the thermally triggered SM polymers into electroactive, magneto-active, photo-active, or water-active SM composites. Particularly, the addition of carbon nanotubes (CNTs) into thermal-responsive polymers converts them in electroactive

* Corresponding author.
E-mail address: silvia.gonzalez@urjc.es (S.G. Prolongo).

https://doi.org/10.1016/j.eurpolymj.2021.110888
Received 25 June 2021; Received in revised form 14 November 2021; Accepted 17 November 2021
Available online 27 December 2021

SM composites by Joule's heating. The resistive Joule intrinsic heating has numerous advantages [7] as compared with direct external heating. It is a fast, convenient, uniform and remotely controllable heating.

Several works have been published about the electroactive thermosetting SM nanocomposites doped with CNTs [11–14]. The formation of an electrical percolation network of nanotubes into the electrically insulator polymer matrix increases the electrical conductivity of nanocomposites, allowing their resistive heating by Joulés effect. In this way, nanocomposites can be electrically triggered with high heating efficiency and without adversely influencing the SM behaviour [14].

Recently, several design strategies have been investigated to broaden their horizons, so increasing their versatility and performance. For example, Li et al. [15] designed an electrically stimulated SM double-layer composite structure for developing a bidirectional actuator in which the SM process is dominated by the temperature-dependent exerting force from the top and bottom layers, alternately. In this way, they built an inchworm-type robot whose locomotion is realised by such bidirectional SM. De la Flor et al. [5] also developed a free-standing thermally triggered two-way SM actuator based on multilayer structures of glassy thermoset anchored to a programmed liquid crystalline network film. These materials are reversible bidirectional actuators, able to bend and unbend various consecutive heating–cooling treatments. On the other hand, Yang et al. [1] synthesised a reversible SM polymer based on a blend of thermosetting resins with a thermoplastic copolymer, where CNTs were segregated on a specific polymer phase, developing electro and light stimulated SM actuators as multi-responsive robots.

In this work, we propose to develop a conventional dual-shape thermally triggered SM resin (one permanent shape and one temporary shape) into an electrothermally stimulated SM thermoset, able to fix several stable temporary shapes, by CNT addition and the design of the electrode network. In this way, sequential and selective actuators have been developed with electrical remote control. This strategy could be applied for any SM polymer system. For reasons of simplicity, the traditional amine-cured epoxy resins were manufactured with different aromatic amines at off-stoichiometry [16] in order to tailor their viscoelastic properties, and therefore their SM behaviour.

2. Experimental section

2.1. Materials

The epoxy monomer used was diglycidyl ether of bisphenol A (DGEBA, Sigma Aldrich), with a molecular weight per epoxy equivalent of 170.2 g/eq, which was dried at 80 °C under vacuum for several hours prior to manufacture. Diaminodiohenylsulfone (DDS) and 4,4′diamine-diphenylmetane (DDM), both supplied by Sigma Aldrich, were used as aromatic amine hardeners. Multiwalled CNT (NC7000, Nanocyl) presented an average diameter and length of 9.5 nm and 1.5 m, respectively. Their specific surface is in the range of 250–300 m^2/g and their purity is higher than 90 %. Their volumetric electrical conductivity, measured by the supplier, is 10^6 S/m.

2.2. Sample preparation

Stoichiometric (R = 1) and off-stoichiometric (R = 1.8) resins were manufactured, where R is the ratio between epoxy groups from DGEBA and amine hydrogen from hardeners, corresponding to epoxy:hardener weight ratios of DGEBA:DDS (100:36 and 100:20) and DGEBA:DDM (100:29 and 100:16). Neat epoxy networks and nanocomposites, doped with a CNT percentage higher than the electrical percolation network, 0.2 wt%, were manufactured. CNT dispersion into DGEBA was carried out with a three-roll mini-calendar (Exakt 80E) at 40 °C, using a previously optimised dispersion procedure [17]. The electrode network, constituted by previously ground copper wires of 1.50 mm, was located over the surfaces of samples using silver paint as a non-resistive glue.

The applied curing treatment was 210 °C for 3 h for samples based on DGEBA:DDS system, and 100 °C for 1 h, followed by a post-curing treatment at 150 °C for 2 h for DGEBA:DDM system [16].

2.3. Characterisation

Thermal characterisation. The Tg of the stoichiometric and non-stoichiometric DGEBA:DDS and DGEBA:DDM resins and composites was determined by Differential Scanning Calorimetry (DSC, Mettler 822e). Two dynamic DSC scans were performed at 10 °C/min from −20 to 280 °C, following the standard ASTM E1356.

Electrical characterisation. Electrical behaviour was studied using an electrical source meter (Keithley 2410), according to ASTM D4496. The transported current was measured by the application of different constant voltages, from 0 to 400 V, using squared thin specimens (10 × 1 × 10 mm^3), with a compliance of 20 mA.

Thermoelectrical characterisation. A thermal camera (FLIR E50) coupled and synchronised up to a current source meter (Keithley 2410) was used to determine the resistive heating by Joulés effect. Different constant voltages, from 50 to 500 V, were applied over the samples, determining the average and the maximum temperature reached with respect to room temperature.

Shape memory characterisation. The shape fixity and recovery ratios were determined by a U-type test [18,19]. SM test was performed with rectangular specimens (2 × 5 × 60 mm^3), according to the following steps: (1) The initial bending angle was recorded as (initial angle). Samples were heated up to the transition temperature, which was fixed as the glass transition temperature of the network plus 10 °C (Tg + 10 °C), using a convection oven or applying a specific electrical voltage in the case of the Joule's heating specimens. (2) The samples were bent into U-shape moulds with 90° and 180° (stored angle), corresponding with a curvature radius of 38 and 19 mm, respectively. Then, the U-shaped specimens were cooled at room temperature and removed from the mould. The bending angle, fixed after 2 h at room temperature, was recorded as (fixed angle). 3) U-shaped specimens were again heated up to the transition temperature at which they were previously deformed. SM recovery was observed, and the bending angle of the final specimens was collected as (recovered angle). All previously mentioned angles were measured with regard to . The shape fixity ratio (SF) and shape recovery ratio (SR) were calculated by the expressions (1) and (2), respectively.

$$S_F(\%) = (1 - \frac{\theta_s - \theta_F}{\theta_s}) \cdot 100 \quad (1)$$

$$S_R(\%) = \frac{\theta_F - \theta_R}{\theta_F} \cdot 100 \quad (2)$$

The study and evaluation of sequential and selective SM behaviour is based on the U-shape test using the same rectangular specimens but locating several electrodes along the length of the sample to induce the shape recovery with selective remote control. In this way, a conventional dual-shape memory thermoset network is turned into a sequentially and selectively triggered shape memory nanocomposite, able to deploy several stable temporary shapes.

3. Results and discussion

3.1. Thermal characterisation: determination of the SM transition temperature.

Table 1 shows the Tg of the studied samples measured during the first and second DSC scans in order to determine the SM transition temperature (Tg + 10 °C). As was expected, the Tg of stoichiometric resins is higher for the resin cured with DDS. In fact, the DGEBA:DDS system is the basic formulation for aeronautical composites, which requires high thermal strength. The breakage of the stoichiometry induces an

Table 1
Glass transition temperature measured by DSC.

Sample*	wt.%CNT	R	Mass (g)				Tg1 (°C)**	Tg2 (°C)**
			DGEBA	DDM	DDS	CNT		
R1-M	0.0	1.0	100	29	–	–	155.29	179.38
C1-M	0.2	1.0	100	29	–	0.25	154.92	176.20
R1.8-M	0.0	1.8	100	16	–	–	62.10	62.54
C1.8-M	0.2	1.8	100	16	–	0.20	68.10	74.02
R1-S	0.0	1.0	100	–	36	–	160.75	219.71
C1-S	0.2	1.0	100	–	36	0.27	160.05	205.10
R1.8-S	0.0	1.8	100	–	20	–	97.83	122.05
C1.8-S	0.2	1.8	100	–	20	0.24	104.20	122.13

*R and C corresponds with resins (0.0 wt% CNT) and composites (0.2 wt% CNT), respectively.
*The different epoxy/NH ratios were 1 (stoichiometric ratio) and 1.8 (amine defect).
*M and S indicates the amine hardener used, DDM and DDS, respectively.
**Tg1 and Tg2 is the glass transition temperature of the network measured by the onset of transition during the first and second DSC scans, respectively.

important reduction of the Tg due to the lower crosslinking density of the network associated to a lower epoxy group conversion. This allows evaluating the influence of the crosslinking degree on their SM behaviour, comparing the resins with different epoxy/NH ratios, and the effect of stiffness due to the use of different amine hardeners. Finally, CNT addition scarcely affects the Tg of the network.

3.2. Electrical and electrothermal characterisation: determination of the applied voltage to reach the SM transition temperature by Joule effect

During the electrical characterisation of the nanocomposites, all the studied samples followed
Ohḿs law:

$$V = I \cdot R \tag{3}$$

There is a linear relationship between the current (I) and voltage (V) at least up to 400 V, as shown in Fig. 1a. Fig. 1b collects the electrical conductivity of the different manufactured nanocomposites, calculated from the I-V slope and the dimensions of the specimens used during the electrical conductivity tests. The CNT percentage added, 0.2 wt%, is higher than the percolation threshold since all nanocomposites present an important increment of several orders of magnitude on their electrical conductivity (in the range of 0.1–1.0 S/m) with regards to insulating neat epoxy resins ($<10^{-9}$ S/m).

It is worthy to note that the electrical conductivity of epoxy resin cured with DDM is higher than the one cured with DDS by one order of magnitude. Moreover, the off-stoichiometric nanocomposites (R = 1.8), which must present the same CNT dispersion degree, show an important increment of their electrical conductivity with regards to stoichiometric samples (R = 1). This fact clearly means that the least stiff and crosslinked networks present higher electrical conductivities with CNT addition due to the weaker physical interaction between the surrounded insulating matrix and the electrically conductive nanotubes, enhancing the direct electrical contact and tunnelling effect between CNTs which are the main electron transport mechanisms implied in the percolated network of nanotubes.

There are numerous published works [20–22] about the influence of the content, aspect ratio, and size of electrically conductive nanofillers, and even their dispersion degree into polymer matrix on the electrical conductivity and the percolation threshold. Moreover, the effect of functionalisation of nanofillers, which strengthens the interface so enhancing the load transfer and increasing the mechanical properties but decreasing the electrical conductivity due to the stronger covalent bond interaction with the surrounding matrix so hindering the direct contact between electrical nanofillers, has been widely studied. However, although it is known [20] that the nature and crosslinking density of the epoxy matrix can significantly affect the interface with the nanofillers, its effect on the electrical behaviour is less studied. Bauhofer and Kovacs [20] confirmed that the thickness and the electrical conductivity of the interphase layer, surrounded by nanotubes, can play the tunnelling effect. The thickest interphase causes the highest conductivity due to the interphase around the nanoparticles playing the tunnelling effect which controls the electrical conductivity where nanotubes are electrically connected. Our results confirm that the densely crosslinked epoxy networks with higher values of Tg present much lower electrical conductivity due to the broader and stronger interphase around the

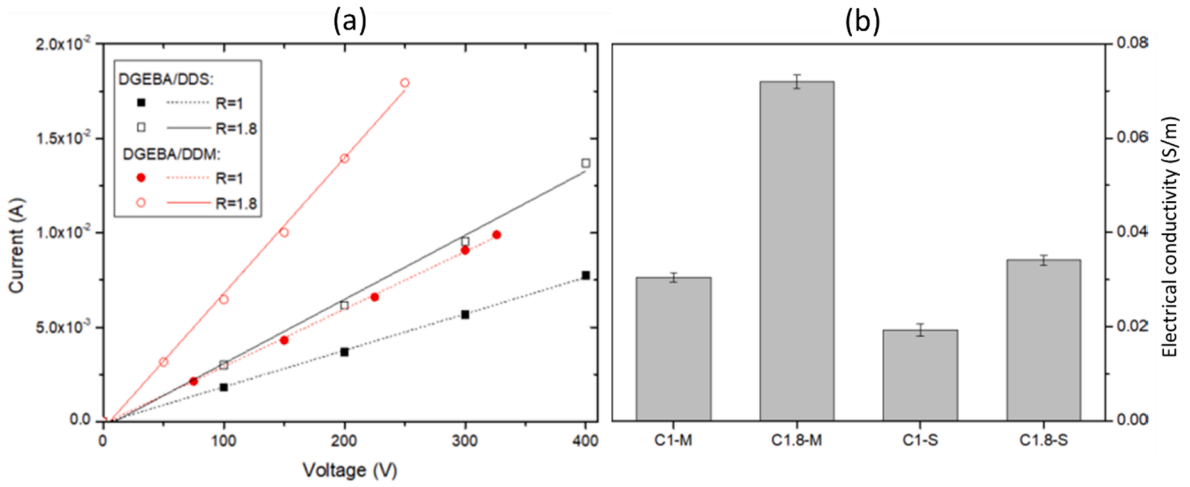

Fig. 1. Electrical characterisation of epoxy/CNT nanocomposites: (1a) I-V curves and (1b) electrical conductivity.

nanotubes.

The thermoelectrical behaviour of the nanocomposites was studied by the application of constant voltage followed by the measurement of temperature increment with respect to room temperature due to Joulés heating. The heat dissipation, Q, in a certain time, t, is correlated to the electrical resistance, R, and the current flow across the material, I, following the well-known Joule's law:

$$Q = I^2 \cdot R \cdot t \tag{4}$$

In this way, knowing that the nanocomposites follow the Ohms law, it is deduced that the increment of temperature (T) caused by the application of constant voltage (V) must be proportional to the squared voltage:

$$\Delta T \alpha \frac{v^2}{R} \tag{5}$$

Fig. 2 shows the average temperature reached as a function of the square of applied voltage, confirming the linear relationship. As was expected, the slope increases as the electrical conductivity of the nanocomposites increases, due to the lower electrical resistance and therefore higher current transported.

Moreover, changing the amine hardener and even the amine/epoxy stoichiometry, it is possible to customise the thermal (Tg in the range of 62 to 220 °C), electrical (conductivity in the range

of 0.01 to 0.08 S/m) and thermoelectrical (reaching from 55 to 130 °C at 200 V) properties of nanocomposites, keeping the rest of experimental parameters, such as CNT percentage added which could affect the dispersion degree and the viscosity of the uncured mixture so modifying the final CNT network, constant. In the studied nanocomposites, the CNT dispersion degree reached, and therefore, the CNT network generated, must be similar because the same percentage of nanotubes is dispersed in the same epoxy monomer. In this way, the possibility of tailoring SM resins with different glass transition temperatures and different crosslinking degrees allows to study the relationship between their SM behaviour and the network structure, in addition to the hindering effect of nanofillers on the SM phenomenon.

3.3. Shape memory characterisation

Once the thermal, electrical and thermoelectrical behaviour is determined, the shape memory (SM) is analysed by conventional heating in a convection oven and, on the other hand, by electrical resistive heating by Joulés effect.

Fig. 3a and 3b show the shape fixity and recovery ratios,

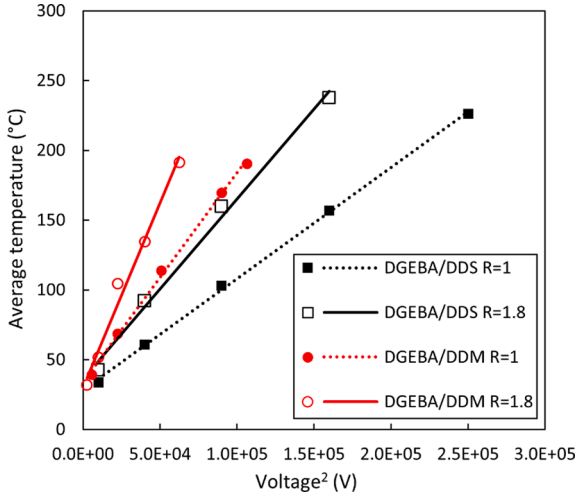

Fig. 2. Thermo-electrical characterisation of epoxy/CNT nanocomposites: Variation of average temperature as a function of the square of voltage.

respectively, measured for neat epoxy resins as a function of the initial deformation degree of the U-mould, 90 and 180. Here, SM is thermally activated in a convection oven at Tg + 10 °C. For all studied samples, the SF is in the range of 75–90% while the SR is around 93–99%, which agrees with the published results for similar resins [16]. No great differences are observed between the samples.

It is well known that the SF mainly depends on the activation temperature [23], but the programming temperature applied in this work was always above the glass transition temperature of each resin. The breakage of the stoichiometry induces an increment of the SF due to the lower crosslinking degree of the network. This effect is more evident for the less stiff resin, which is cured with DDM. In this regard, the same above mentioned explanation justifies the higher SF of the DGEBA/DDM system with regards to DGEBA/DDS. Therefore, as was expected [4], the shape fixing ratio is enhanced with the reduction of crosslinking degree.

It is worthy to note the change of tendency between both studied systems as a function of the initial bending angle of the mould. The stiffer resin, DGEBA/DDS, has a better shape fixation with the mould with higher curvature, 180°, while the DGEBA/DDM system has a higher SF for the lower initial bending angle, 90°. This is associated with the ability of energy storing. The less crosslinked resin, DGEBA/DDM, can store more energy at lower bending forces while the stiffer resin requires more deformation.

The SR is very high, close to 100 %, in all studied samples, being slightly lower for the off-stoichiometric resins, especially for the high initial angle. This is associated to the more heterogeneous network due to low epoxy conversion reached. De la Flor et al. [24] studied the dependence of shape recovery process on the network structure, particularly on the network relaxation process with dual-curing off-stoichiometric thiol-epoxy resins, and they confirmed that the heterogeneous network structures present lower recovery rates. As is mentioned above, the off-stoichiometric resins present a lower crosslinking degree, and this implies lower shape recovery.

Fig. 4 shows the comparison of shape fixity and recovery ratios for neat epoxy resins and nanocomposites doped with 0.2 wt% CNT.

In spite of the stiffness increase, CNT addition scarcely affects the shape memory cycle. Moreover, the temporary shape can be fixed with a relatively high efficiency (SF ranging from 75 to 90%), similar to other studies using similar materials [25–27]. However, the SR of nanocomposites is lower than the corresponding neat resins, indicating less stored energy during the shaping due to the lower free mobility caused by the steric hindrance of the nanofillers. Zhong et al. [23] confirmed that the recovery efficiency was not improved by CNT, requiring a higher programming temperature. However, their recovery stress is much larger than the SM polymers due to their enhanced mechanical properties [23,24]. Moreover, the CNT addition could also speed up the shape recovery of thermosensitive polymers due to the enhancement of heat transfer [10].

The main advantage of CNT addition on SM networks is their use as electro-activated SM resins, allowing their remote control [10]. Joulés heating is induced by the electrical current passing through the conductive CNT network within the polymer matrix, implying an internal volumetric heating which reduces the temperature gradient from the surface.

Fig. 5 presents the shape fixity and recovery ratios of nanocomposites electrically triggered by remote control in comparison with the convection heating in an oven. The switching temperature was always Tg + 10 °C, which, in the case of the Joule's heating specimens, is reached by the application of a constant voltage in the range of 126 to 265 V, depending on the glass transition temperature of the matrix (Table 1) and its electrical conductivity (Figs. 1 and 2).

The SF seems not to depend on the heating mode. The main difference is the time required. The stable temporary shape is fixed at 20–30 min in a convection oven while the same shape is achieved in less than 5 min by Joulés heating. Moreover, the programming time by electro-resistive heating decreases for lower bending strain using a U-mould

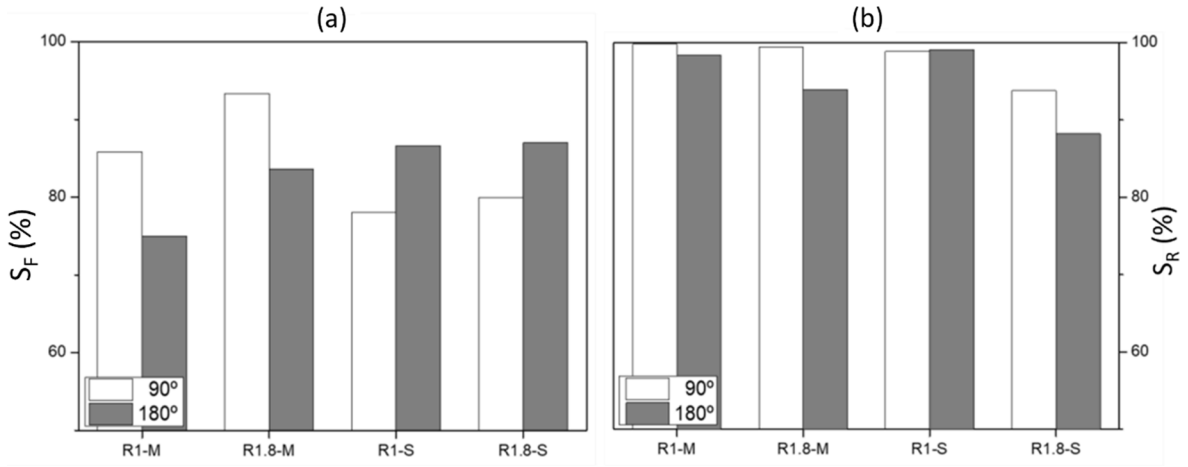

Fig. 3. Shape fixity (3a) and recovery (3b) ratios for neat epoxy resins as a function of initial bending angle of the U-mould: 90° and 180°.

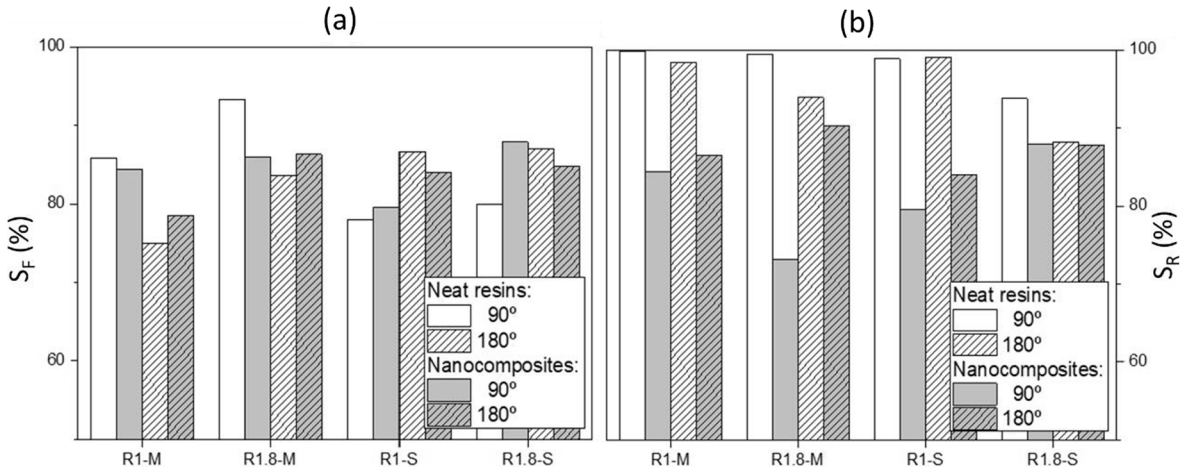

Fig. 4. Shape fixity (4a) and recovery (4b) ratios for neat epoxy resins and nanocomposites doped with 0.2 wt% CNT as a function of initial bending angle of the U-mould.

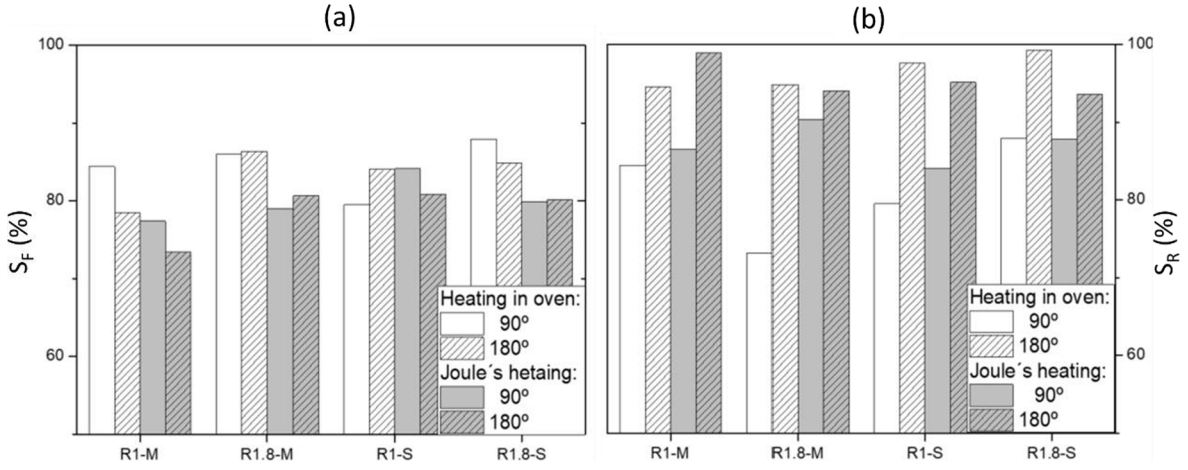

Fig. 5. Shape fixity (5a) and recovery (5b) ratios for nanocomposites doped with 0.2 wt% CNT thermally triggered by convection and electro-resistive heating as a function of initial bending angle of the U-mould.

with a lower initial angle. The most important point is the wide increment on SR through resistive heating. In fact, the SR reached by Joule's heating for composites are close to 85–100%, similar to neat epoxy resins, recovering the lost efficiency by CNT addition. These results are in total agreement with other similar studies using thermoelectrically activated SM composites embedding CNTs [26,28,29]. The main reason for this important enhancement is the internal heating induced by Joulés effect. The internal CNT network is intrinsically heated by the current

transport within the SM matrix without thermal gradient losses from the surface.

As an example, Fig. 6 shows the evolution of shape recovery and the increase of temperature reached with the time of electrical voltage application for several nanocomposites with different initial temporal shapes, deformed with 90° or 180° U-mould. In all cases, the shape recovery starts before 1 min, the time required to reach the switching temperature. The final time to achieve the permanent shape is in the range of 3–5 min, being lower for the least bent temporary shapes with an initial angle of 90°. However, the final SM recovery time scarcely depends on the crosslinking degree of the epoxy network. This is explained because the switching temperature is always above the glass transition temperature of the matrix, Tg + 10 °C. It is worthy to note that the evolution of the shape recovery occurs in only one stage for the least bent samples, using 90° U-mould, while this phenomenon seems to occur in several stages for the samples whose initial deformation angle is 180°. However, the different temporary shapes formed during the thermo-electrical recovery are not constant because they depend on the CNT distribution on the electrical network and therefore, undergo not totally homogenous heating as is confirmed on the thermographic IR images. On the other hand, as was expected, the final shape recovery ratio reached is very high and depends on the chemical nature of the resin matrix as was explained before (Fig. 5).

Once the high SM efficiency by Joulés heating, whose main advantages are greater speed, remote control and extension of their potential applications due to easier industrial and daily life implementation, has been confirmed, the selective and sequential shape memory process has been developed. For self-deployable structures and packaging, the abrupt recovery of the whole permanent shape imposes certain constraints. Fig. 7 shows the curves of Joulés heating and SR as a function of the time when a constant voltage is applied. At the right of these curves, photographs of selectively and remotely controlled self-deployable samples are shown at different stages, with two different temporary shapes and the final permanent shape developed with time. For this experiment, several parallel electrodes are included in different regions of the samples, which are selectively activated when the corresponding segment has to be deployed.

These obtained results confirm that the electro-resistive heating allows a high control of temporary shapes, turning a conventional dual-shape SM resin into a remotely and selectively triggered SM nanocomposite, able to store several temporary shapes as desired.

The different temporary shapes are controlled, and they are maintained even at room temperature. The SR is also very high in each thermo-electrical segment, close to 90–100 % with regard to the

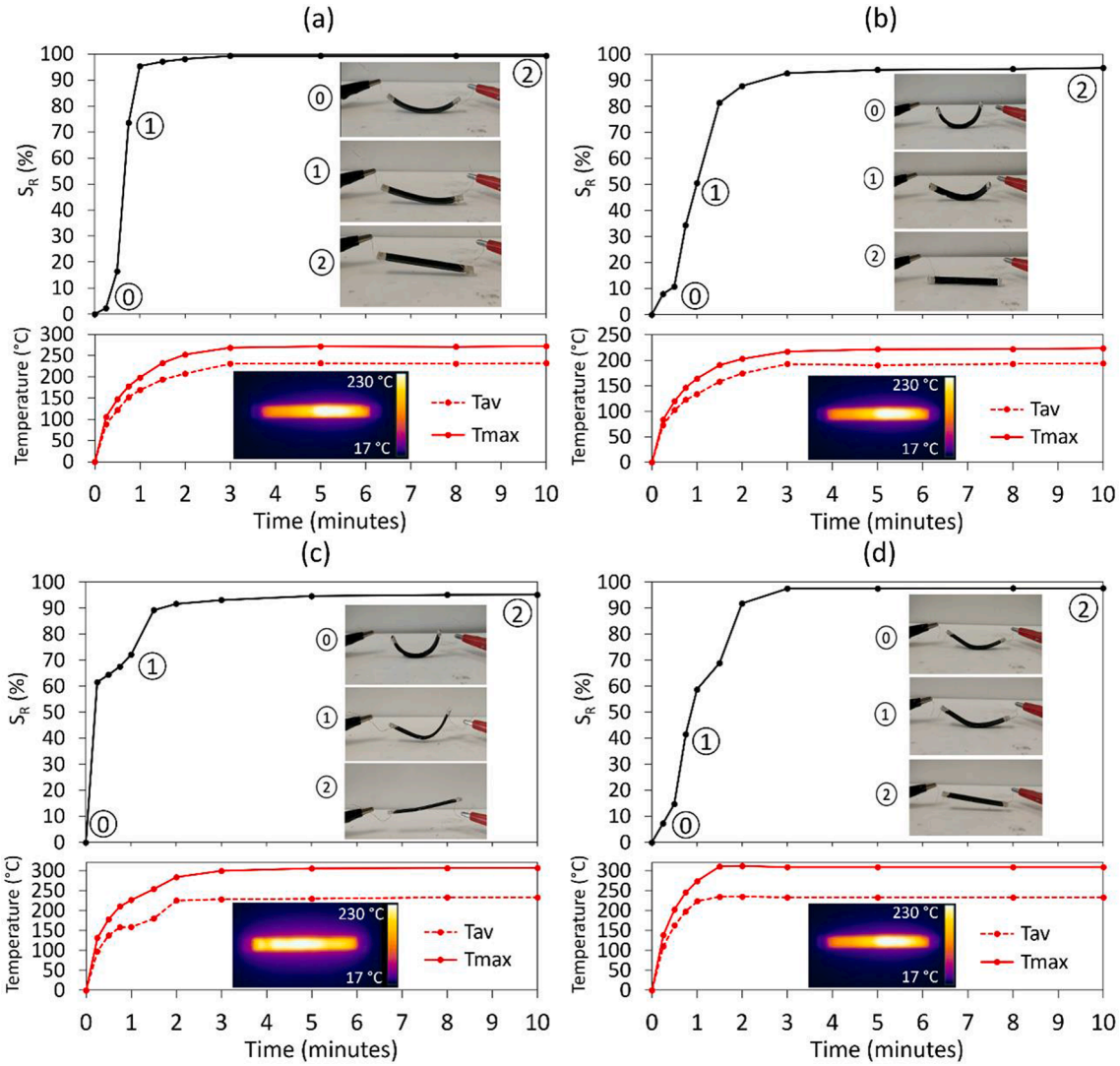

Fig. 6. Variation of shape recovery (SR), maximum (Tmax) and average (Tav) temperature reached with the time of electrical voltage application (left), and photographs of temporary and permanent shapes (right) for several nanocomposites with different initial deformation angles: (6a) R1.8-S with 90°; (6b) R1-M with 180°; (6c) R1-S with 180°; (6d) R1-S with 90°.

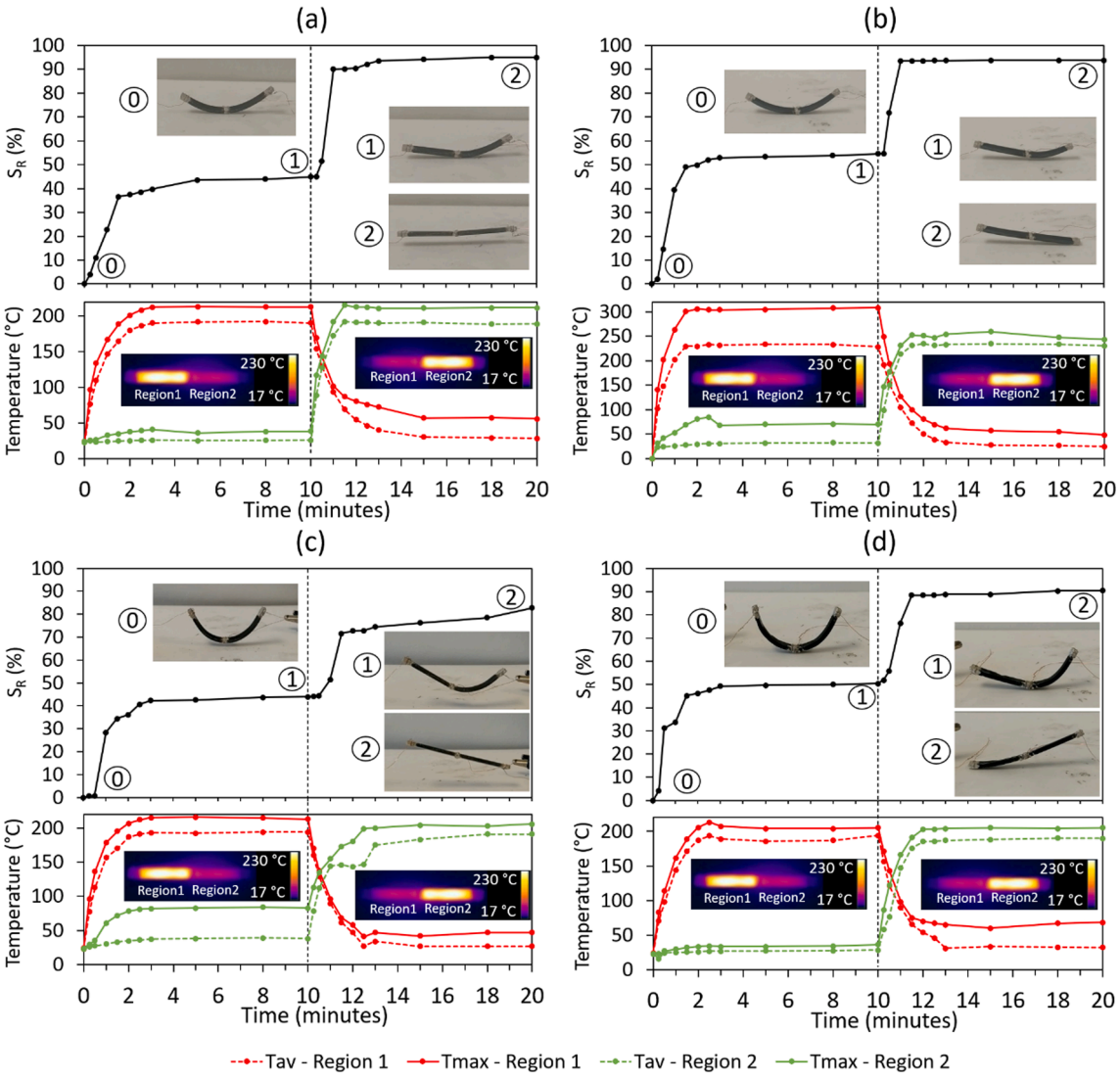

Fig. 7. Gradual shape recovery ratio remotely and selectively controlled by Joulés heating for different nanocomposites with different initial deformation angles: (7a) R1-S with 90; (7b) R1.8-S with 90; (7c) R1-M with 180 and (7d) R1.8-M with 180.

previous results presented (Fig. 5). In this experiment, the recovery time per segment is lower than 2 min. In fact, the shape recovery is almost instantaneous when the temperature reaches the selected switching temperature. This means that the SM speed corresponds with Joulés heating speed. This is due to the distance between electrodes being half that of the previous experiment (Fig. 6). This means that the recovery time strongly depends on the distances between the electrodes in spite of the Joulés heating remaining constant. For a distance between electrodes of 50 mm, the recovery time for all studied nanocomposites is close to 5 min for U-bent shapes with an initial angle of 180 (Fig. 6b, 6c and 6d) in spite of the switching temperature being reached in the first two minutes. When the distance between electrodes is halved, 25 mm, the recovery is instantaneous when the switching temperature is reached at 2 min. This means that the shape memory phenomenon with intrinsic heating, such as electro-resistive heating, requires more time depending on the size of the sample.

4. Conclusions

CNT addition on epoxy resins increases their electrical conductivity, allowing their self-heating by Joulés effect through the application of an electrical DC voltage. The temperature reached by electrical resistive heating is lineally proportional to the square of the applied voltage. On the other hand, the breakage of epoxy/amine stoichiometry in epoxy resins allows tailoring the glass transition temperature and, therefore, the SM behaviour since the switching temperature is above Tg.

The SF in stoichiometric and off-stoichiometric epoxy resins is in the range of 75–90%, being higher with the reduction of the crosslinking degree of the network. However, the shape recovery is close to 100%, being lower for off-stoichiometric resins due to their more heterogeneous network. CNT addition scarcely affects the SF. However, CNT addition reduces the SR due to lower stored energy on the temporary shapes associated to lower free mobility caused by the steric hindrance induced by CNTs. The main advantage of CNT addition on thermosensitive polymers is the ability to perform the shape memory cycle by electrical activation. In our studied nanocomposites, the voltage required is in the range of 126–265 V in order to reach a temperature equal to Tg + 10 °C. The electrical resistive heating is faster than convection due to the intrinsic heating of the CNT network within the polymer matrix due to the current transport, without a temperature gradient from the surface. In fact, the Joulés heating significantly enhances the SR.

Finally, the Joulés heating of nanocomposites allows a fast and efficient SM process with remote control. Moreover, the Joule heating capability due to the CNT addition, together with the proper configuration of several electrodes, turns a conventional dual-shape SM resin

into a remotely and selectively triggered SM nanocomposite, able to store several temporary shapes as desired, which enhances their application as self-deployable structures.

Funding

This work was supported by the Ministerio de Economía y Competitividad of Spain Government [PID2019-106703RB-I00]; and Comunidad de Madrid Government [ADITIMAT-CM S2018/NMT-4411].

CRediT authorship contribution statement

A. Cortés: Formal analysis, Writing – review & editing. **N. Pérez-Chao:** Investigation. **A. Jiménez-Suárez:** Methodology, Investigation. **M. Campo:** Resources, Project administration, Funding acquisition. **S.G. Prolongo:** Conceptualization, Formal analysis, Writing – original draft, Resources, Supervision, Funding acquisition.

Declaration of Competing Interest

The authors declare that they have no known competing financial interests or personal relationships that could have appeared to influence the work reported in this paper.

References

[1] Z. Xu, C. Ding, D.-W. Wei, R.-Y. Bao, K. Ke, Z. Liu, M.-B. Yang, W. Yang, Electro and light active actuators based on reversible shape-memory polymer composites with segregated conductive networks, ACS Appl. Mater. Interfaces 11 (33) (2019) 30332–30340.
[2] M. Shahinpoor, Ionic polymer–conductor composites as biomimetic sensors, robotic actuators and artificial muscles—a review, Electrochim. Acta 48 (14-16) (2003) 2343–2353.
[3] Y. Wu, Y. Wei, Y. Ji, Polymer actuators based on covalent adaptable networks, Polym. Chem. 11 (33) (2020) 5297–5320.
[4] J. Karger-Kocsis, S. Kéki, Review of progress in shape memory epoxies and their composites, Polymers 10 (2018) 34.
[5] A. Belmonte, G.C. Lama, G. Gentile, P. Cerruti, V. Ambrogi, X. Fernández-Francos, S. De la Flor, Thermally-triggered free-standing shape-memory actuators, Eur. Polym. J. 97 (2017) 241–252.
[6] K. Kumar Patel, R. Purohit, Future prospects of shape memory polymer nanocomposite and epoxy-based shape memory polymer – a review, Mater. Today:. Proc. 5 (9) (2018) 20193–20200.
[7] H. Meng, G. Li, A review of stimuli-responsive shape memory polymer composites, Polymer 54 (9) (2013) 2199–2221.
[8] Y. Liu, J. Zhao, L. Zhao, W. Li, H. Zhang, X. Yu, Z. Zhang, High performance shape memory epoxy/carbon nanotube nanocomposites, ACS Appl. Mater Interfaces 8 (1) (2016) 311–320.
[9] E. Wang, Y. Dong, MD.Z. Islam, L. Yu, F. Liu, S. Chen, X. Qi, Y. Zhu, Y. Fu, Z. Xu, N. Hu, Effect of graphene oxide-carbon nanotube hybrid filler on the mechanical property and thermal response speed of shape memory epoxy composites, Compos. Sci. Technol. 169 (2019) 209–216.
[10] Q.-Q. Ni, C.-S. Zhang, Y. Fu, G. Dai, T. Kimura, Shape memory effect and mechanical properties of carbon nanotube/shape memory polymer nanocomposites, Compos. Struct. 81 (2) (2007) 176–184.
[11] S. Datta, T.C. Henry, Y.R. Sliozberg, B.D. Lawrence, A. Chattopadhyay, A.J. Hall, Carbon nanotube enhanced shape memory epoxy for improved mechanical properties and electroactive shape recovery, Polymer 212 (2021) 123158.
[12] Z. Zhang, W. Wang, J. Yang, N. Zhang, T. Huang, Y. Wang, Excellent electroactive shape memory performance of EVA/PCL/CNT blend composites with selectively localised CNTs, J. Phys. Chem. C 120 (2016) 22793–22802.
[13] M. Raja, S.H. Ryu, A.M. Shanmugharaj, Thermal, mechanical and electroactive shape memory properties of polyurethane (PU)/poly (lactic acid) (PLA)/CNT nanocomposites, Eur. Polym. J. 49 (11) (2013) 3492–3500.
[14] W. Wang, Y. Liu, J. Leng, Recent developments in shape memory polymer nanocomposites: Actuation methods and mechanisms, Coord. Chem. Rev. 320-321 (2016) 38–52.
[15] Q. Peng, H. Wei, Y. Qin, Z. Lin, X. Zhao, F. Xu, J. Leng, X. He, A. Cao, Y. Li, Shape-memory polymer nanocomposites with a 3D conductive network for bidirectional actuation and locomotion application, Nanoscale 8 (2016) 18042.
[16] W.B. Song, L.Y. Wang, Z.D. Wang, Synthesis and thermomechanical research of shape memory epoxy systems, Mater. Sci. Eng. 529 (2011) 29–34.
[17] R. Moriche, S.G. Prolongo, M. Sánchez, A. Jiménez-Suárez, M.J. Sayagués, A. Ureña, Morphological changes on graphene nanoplatelets induced during dispersion into an epoxy resin by different methods, Compos. Part B: Eng. 72 (2015) 199–205.
[18] K.A. Revathi, S. Rao, S. Srigari, G.N. Dayananda, Characterisation of shape memory behaviour of CTBN-epoxy resin system, J. Polym. Res. 19 (2012) 9894.
[19] K. Wei, G. Zhu, Y. Tang, T. Liu, J. Xie, The effects of crosslinking density on thermo-mechanical properties of shape-memory hydro-epoxy resin, J. Mater. Res. 28 (2013) 2903–2910.
[20] Y. Zare, K.Y. Rhee, Calculation of electrical conductivity of polymer nanocomposites assuming the interphase layer surrounding carbon nanotubes, Polymers 12 (2020) 404.
[21] C. Min, X. Shen, Z. Shi, L. Chen, Z. Xu, The electrical properties and conducting mechanisms of carbon nanotube/polymer nanocomposites: a review, Polym.-Plastics Technol. Eng. 49 (12) (2010) 1172–1181.
[22] W. Bauhofer, J.Z. Kovacs, A review and analysis of electrical percolation in carbon nanotube polymer composites, Compos. Sci. Technol. 69 (10) (2009) 1486–1498.
[23] H. Li, J. Zhong, J. Meng, G. Xian, Xian, The reinforcement efficiency of carbon nanotubes/shape memory polymer nanocomposites, Compos. B Eng. 44 (1) (2013) 508–516.
[24] A. Belmonte, C. Russo, V. Ambrogi, X. Fernández-Francos, S. De la Flor, Epoxy-based shape-memory actuators obtained via dual-curing of off-stoichiometric "thiol–epoxy" mixtures, Polymers 9 (2017) 113.
[25] A. Cortés, J.L. Aguilar, A. Cosola, X.X. Fernández Sanchez-Romate, A. Jiménez-Suárez, M. Sangermano, M. Campo, S.G. Prolongo, 4D-printed resins and nanocomposites thermally stimulated by conventional heating and IR radiation, ACS Appl. Polym. Mater. 3 (10) (2021) 5207–5215.
[26] A. Cortés, A. Cosola, M. Sangermano, M. Campo, S.G. Prolongo, C.F. Pirri, A. Jiménez-Suárez, A. Chiappone, DLP 4D-printing of remotely, modularly, and selectively controllable shape memory polymer nanocomposites embedding carbon nanotubes, Adv. Funct. Mater. Early View (2021) 2106774.
[27] S.A. Abdullah, A. Jumahat, N.R. Abdullah, L. Frormann, Determination of shape fixity and shape recovery rate of carbon nanotube-filled shape memory polymer nanocomposites, Procedia Eng. 41 (2012) 1641–1646.
[28] X. Wan, F. Zhang, Y. Liu, J. Leng, CNT-based electro-responsive shape memory functionalized 3D printed nanocomposites for liquid sensors, Carbon 155 (2019) 77–87.
[29] S. Gu, B. Yan, L. Liu, J. Ren, Carbon nanotube–polyurethane shape memory nanocomposites with low trigger temperature, Eur. Polym. J. 49 (12) (2013) 3867–3877.